CrystEngComm

RSC Publishing

COMMUNICATION

View Article Online
View Journal | View Issue

Cite this: *CrystEngComm*, 2013, **15**, 8933

Received 12th July 2013,
Accepted 10th September 2013

DOI: 10.1039/c3ce41365a

www.rsc.org/crystengcomm

Facile synthesis of novel α-Ag_3VO_4 nanostructures with enhanced photocatalytic activity†

Di Li, Xiaochuan Duan, Qing Qin, Hongmin Fan and Wenjun Zheng*

Novel α-Ag_3VO_4 nanostructures have been successfully synthesized *via* a facile and repeatable precipitation method by using *n*-BA as precipitant and complexing agent. Photocatalytic property tests for decomposition of RhB demonstrate that the as-prepared nanostructures have enhanced photocatalytic activity.

Photocatalytic technology using semiconductors has been regarded one of the most promising methods to address water pollution and the energy crisis.[1–3] As one of the silver vanadate materials, α-Ag_3VO_4 has attracted much attention not only because it is considered as a potential p-type transparent conductor[4] but also because it is able to act as a candidate material for visible light photocatalysts.[5–7] α-Ag_3VO_4 with a monoclinic structure has a narrower band gap (~2.2 eV)[5,8] and can absorb wider solar spectral range than the most studied photocatalysts, such as TiO_2 (~3.2 eV),[9–11] which makes it have greater spectral response and higher utilization of sunlight.

Unlike bulk materials, properties of nanomaterials are strongly dependent on their morphology, for example their size, shape and surface condition, thus there has been increasing interest in controllable synthesis of nanomaterials with unique morphologies.[12–15] In recent years, significant advances in the controlled preparation of nanomaterials have been made.[16,17] Murray and co-workers[18] have reported the controlled synthesis of highly uniform TiO_2 nanocrystals with a size of 10–100 nm *via* a seeded growth technique, and photocatalytic activity tests proved that the photocatalytic properties of the as-prepared photocatalysts are greatly related to the morphology. Yang *et al.*[19] have designed and synthesized anatase TiO_2 single crystals with a large percentage of {001} facets, which is very useful as model single crystals for fundamental studies in surface science. However, to the best of our knowledge, there has been no report in the literature fully investigating α-Ag_3VO_4 with controlled morphology.

Herein, we report a facile precipitation method to synthesize α-Ag_3VO_4 nanostructure with novel and controllable morphologies which $AgNO_3$ was used as Ag resource and *n*-butylamine (*n*-BA) was used as both the precipitant and complexing agent. By adjusting the amount of *n*-BA, α-Ag_3VO_4 nanostars and nanoflowers have been prepared successfully. Moreover, studies of their photocatalytic properties for decomposition of rhodamine B (RhB) have clearly revealed that the as-prepared α-Ag_3VO_4 nanostructures exhibit better photocatalytic behaviours than other reports. It should be noted that this study will fill in a gap in the comprehensive investigation of the morphology, crystal structure and photocatalytic activity of α-Ag_3VO_4 nanostructures, and also can offer a strategy toward preparing a visible-light photocatalyst with a simple, low-cost and repeatable method, which may realize the large-scale production of the photocatalyst.

The detailed experiments and characterization methods are listed in the ESI.† The XRD pattern of α-Ag_3VO_4 nanostars and standard pattern are shown in Fig. S1a.† The insert shows the schematic illustration of the unit cell of the monoclinic α-Ag_3VO_4 structure. It can be found that the as-prepared α-Ag_3VO_4 nanostars show a highly crystalline and monoclinic phase of α-Ag_3VO_4 with cell parameter constants a = 10.1885 Å, b = 4.9751 Å, c = 10.2014 Å, β = 115.754°, and space group $C2/c$ (No. 15) (ICSD # 249417).[20] The intensities of XRD peak correlate well with those from the standard pattern of α-Ag_3VO_4, and no other peaks ascribed to the impurities can be found,

Department of Materials Chemistry, Key Laboratory of Advanced Energy Materials Chemistry (MOE), and TKL of Metal and Molecule-Based Material Chemistry, College of Chemistry, Nankai University, 94 Weijin Road, Tianjin, 300071, People's Republic of China

† Electronic supplementary information (ESI) available: Detail experimental procedures, photocatalytic activity measurement and recycle photocatalytic experimental process, XRD patterns of as-prepared α-Ag_3VO_4, SEM images of nanostars with different directions, XRD patterns of the α-Ag_3VO_4 crystal under visible light with different irradiation time, SEM image and XRD pattern of Ag_2O, SEM images of samples obtained with different amount of Na_3VO_4 and SEM image of α-Ag_3VO_4 nanoparticles, degradation curves of RhB over as-prepared photocatalysts reusing three times and XRD patterns of the reused photocatalysts. See DOI: 10.1039/c3ce41365a

proving the product is pure phase. The abundance and microstructure of the nanostars have been examined by SEM and TEM. The nanostars exhibit uniform size and regular morphology and the average size is ~350 nm (Fig. 1a and 1b). As shown in Fig. S2,† the detailed architecture of the nanostars is illustrated by an individual sample from different orientations (Fig. S2a to S2d†) and the three-dimensional shape simulated images (Fig. S2a' to S2d'†) corresponding to the SEM images. From the detailed illustrations, we can conclude that the nanostars are assembled by four pyramids which are near in-plane and another pyramid inserts into the intersection of the four pyramid monomers. Though the α-Ag_3VO_4 crystal is stable under visible light irradiation (the XRD patterns of the α-Ag_3VO_4 crystal under visible light with different irradiation times are shown in Fig. S3†), the α-Ag_3VO_4 crystal is unstable under the high energy electron beam in the HRTEM atmosphere and it is difficult to get a HRTEM picture. However, the possible exposed crystal planes of nanostars can be speculated from the XRD pattern, SEM images and the crystal structure of α-Ag_3VO_4. As shown in the XRD patterns, the intensity ratio of (312) to (112) peaks for the product is obviously higher than the standard ratio, suggesting that the facades of the nanostars may be bounded by {312} facets.[21] The dihedral angles of the pyramids' top and bottom are 56.8° and 46.3° obtained from the SEM image (Fig. 1c), which are consistent with the simulation of crystal structure values, 57.2° and 44.7° (Fig. 1d), respectively. Therefore, it can be determined that the monomers of the nanostars may be bound by $(\bar{3}\bar{1}2)$, $(\bar{3}12)$, $(3\bar{1}2)$ and (312) surfaces.

As an organic amine, *n*-BA not only can be used as alkalinity regulator but also can act as a complexing agent to combine with Ag^+ to form Tollens-reagent at an appropriate amount. Tollens-reagent is often employed as an Ag source to synthesise Ag or Ag compounds owing to the slow release of Ag^+ from the complex $[Ag(NH_3)_2]^+$ and can decrease the reaction rate and provide a mild reaction condition.[22,23] During our fabrication process, α-Ag_3VO_4 nanoflowers have been obtained by increasing the amount of *n*-BA when the Tollens-reagent formed. The XRD pattern is shown in Fig. S1b.† As shown in the low magnification SEM image (Fig. 2a), the nanostructures are formed as flower-like assemblies with a mean diameter of ~0.6 μm. It is also can be noticed that the products exhibit uniform morphology, extremely good dispersion and narrow size distribution. The nanoflowers are assembled by irregular pyramids (*ca.* 100 nm) in a random fashion, which is clearly seen in the high magnification SEM image (Fig. 2b). The TEM image (Fig. 2b') also shows typical flower-like structures constructed by small particle units.

The reaction process of the products could be described by the following equations:

$$n-\mathrm{BA}+\mathrm{H_2O}\rightarrow n-\mathrm{BA}\text{–}\mathrm{H^+}+\mathrm{OH^-} \quad (1)$$

$$\mathrm{Ag^+}+2\mathrm{OH^-}\rightarrow \mathrm{Ag(OH)_2^-} \quad (2)$$

$$2\mathrm{Ag(OH)_2^-}\leftrightarrow \mathrm{Ag_2O}+\mathrm{H_2O}+2\mathrm{OH^-} \quad (3)$$

$$\mathrm{VO_4^{3-}}+\mathrm{H_2O}\rightarrow \mathrm{HVO_4^{2-}}+\mathrm{OH^-} \quad (4)$$

$$3\mathrm{Ag(OH)_2^-}+\mathrm{HVO_4^{2-}}\rightarrow \alpha-\mathrm{Ag_3VO_4}+5\mathrm{OH^-}+\mathrm{H_2O} \quad (5)$$

$$\mathrm{Ag_2O}+4(n-\mathrm{BA})+\mathrm{H_2O}\rightarrow 2\mathrm{Ag}(n-\mathrm{BA})_2^++2\mathrm{OH^-} \quad (6)$$

$$3\mathrm{Ag}(n-\mathrm{BA})_2^++\mathrm{HVO_4^{2-}}+5\mathrm{H_2O}\rightarrow \alpha-\mathrm{Ag_3VO_4}+6(n-\mathrm{BA}\text{–}\mathrm{H^+})+5\mathrm{OH^-} \quad (7)$$

In the formation of α-Ag_3VO_4 nanostars, $Ag(OH)_2^-$ was firstly formed after the addition of *n*-BA since the OH^- concentration in the reaction system was high enough to precipitate Ag^+ out from solution (K_{sp}, AgOH = 2×10^{-8}). $Ag(OH)_2^-$ was unstable and rapidly decomposed to Ag_2O when the pH value of the solution was maintained at 8.84. The ionic species in the Na_3VO_4 aqueous solution were not Na^+ and VO_4^{3-} but rather Na^+, OH^- and HVO_4^{2-} at the pH range of 8–13, which has been investigated by Britton and Robinson in the 1930s (eqn (4)).[24] With increasing HVO_4^{2-} concentration,

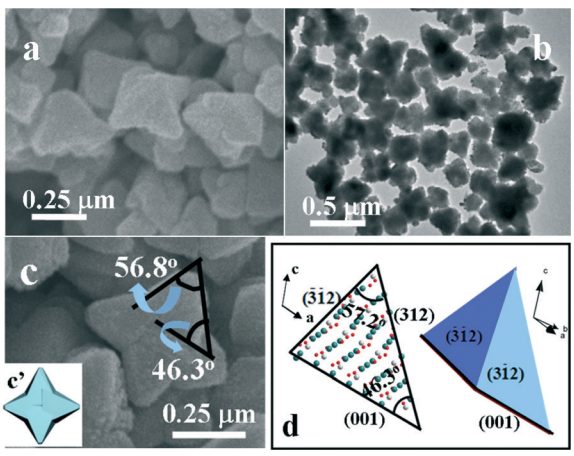

Fig. 1 (a) SEM and (b) TEM images of the synthesized α-Ag_3VO_4 nanostars, (c) SEM image and the geometric model of the single α-Ag_3VO_4 nanostar (inset), (d) schematic illustration of the crystal structure (left) and the geometric model of single nanostars' monomer (right).

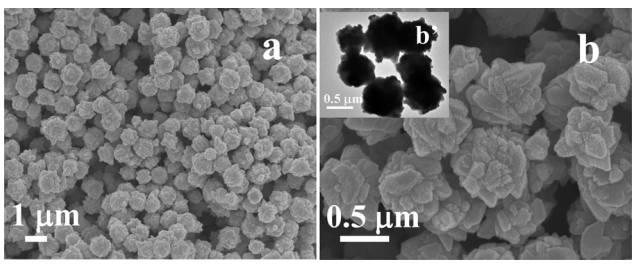

Fig. 2 (a) Low magnification SEM image, (b) medium magnification SEM image and inset (b') is TEM image of α-Ag_3VO_4 nanoflowers.

Ag_2O precipitation dissolved gradually, induced by the alkaline environment, and then a complex composed of Ag^+ and OH^- appeared. Subsequently, α-Ag_3VO_4 was formed by the reaction of $Ag(OH)_2^-$ and HVO_4^{2-} due to a higher chemical stablity than β-Ag_3VO_4.[25] In the process of nanoflower formation, with the increasing of *n*-BA concentration, the color of the reaction system turned from dark brown to transparent (eqn (6)). When the system was completely transparent, Tollens-reagent was synthesized at a pH of 10.91, which was attributed to the higher *K*s of the silver amine complex compared with AgOH ($Ks_{Ag(n-BA)2+}$ = 1.05 × 10^7 and Ks_{AgOH} = 1 × 10^4). After the addition of the Na_3VO_4 aqueous solution, α-Ag_3VO_4 was produced by the reaction of Tollens-reagent and HVO_4^{2-} following eqn (7).

On the basis of experimental observation, a possible growth mechanism of α-Ag_3VO_4 nanostructures has been proposed. For synthesis of α-Ag_3VO_4 nanostars, the crystal growth process of nanostars began from the dissolution of Ag_2O cubes with corrosion holes (Fig. S4†) to form α-Ag_3VO_4 nuclei. Then, the nuclei grew gradually and assembled together to decrease the free energy of the system.[26] To compact the product structure, the nanostar structure was obtained. Meanwhile, during the preparation process of α-Ag_3VO_4 nanoflowers, α-Ag_3VO_4 nuclei formed quickly after adding with Na_3VO_4, and then the nuclei grew to form irregular pyramids. With a ripening process, the unconsolidated product transformed to compact nanostar or nanoflower structures.[27] Both processes are schematically shown in Scheme 1. It should be mentioned that the morphology of α-Ag_3VO_4 nanostructure is dependent on two aspects. Firstly, the rate of nucleation may decide the amount and size of the nuclei. Considering the reactions in eqn (3) and (5), the concentration of $Ag(OH)_2^-$ was maintained at a lower level than the concentration of $Ag(n\text{-BA})_2^+$ owing to the shift of the chemical equilibrium. Because the precursor concentration can directly induce the nucleation rate of α-Ag_3VO_4, nucleation from $Ag(OH)_2^-$ would be slower than from $Ag(n\text{-BA})_2^+$, which can cause the seeds of α-Ag_3VO_4 grow larger, and the steric hindrance will restrict the monomers' ability to assemble into nanostar structures. Secondly, owing to the high concentration of the seeds, it was easier to aggregate to reduce the free energy of the system. Furthermore, the adsorption of *n*-BA on the surface of α-Ag_3VO_4 through hydrogen bonding will restrict the nuclei's growth. Therefore, the nanoflowers formed from the higher concentration of *n*-BA exhibited smaller size but a greater number of monomers. Samples with various morphologies obtained with different amounts of Na_3VO_4 (Fig. S5†) also proved the above deduction.

The UV-vis spectra of α-Ag_3VO_4 nanostars, nanoflowers and the nanoparticles (SEM image shown in Fig. S6†) are shown in Fig. 3a. As an indirect semiconductor material, the band gap energies of α-Ag_3VO_4 can be estimated from the plot of transformed Kubelka–Munk function *versus* the energy of exciting light and the band gap energies of α-Ag_3VO_4 nanostars, nanoflowers and the nanoparticles estimated from these intercepts are about 1.90 eV, 1.95 and 2.05 eV,[28] respectively. By comparing the three curves, α-Ag_3VO_4 nanostars have the highest absorbance intensity and the absorption edge shows a small red shift. These discrepancies may be primarily due to different atomic configurations of the different crystal facets, which is similar to the previous reports of AgBr, Ag_3PO_4 and TiO_2.[21,29,30] The photocatalytic activities of the as-prepared α-Ag_3VO_4 nanostructures have been examined by typical experiments of photocatalytic degradation of RhB under visible light. As shown in Fig. 3b, the nanostars show higher activity than the nanoflowers and nanoparticles, which corresponds to the UV-vis spectra. The photocatalytic superiority of the nanostars over the other structures of α-Ag_3VO_4 may be induced by the special architecture[31] (monomers of nanostars enclosed by {312} facets). As a photocatalyst, the stability is of great importance from a practical viewpoint, besides the photocatalytic activity. The stability of the α-Ag_3VO_4 nanostars and α-Ag_3VO_4 nanoflowers were further investigated by performing recycling experiments (Fig. S7†). After three recycles, the structures of the as-prepared photocatalysts did not show significant loss of activity and the XRD patterns of the reused samples showed little change, indicating their relatively high stabilities during photocatalytic degradation of pollutant molecules.

In conclusion, novel and controllable α-Ag_3VO_4 nanostructures with high photocatalytic activities under visible light have been synthesized using a facile method. Studies of their photocatalytic performance indicate that the as-prepared α-Ag_3VO_4 nanostructures, α-Ag_3VO_4 nanostars with the monomers enclosed by {312} facets, particularly, show better photocatalytic activity than α-Ag_3VO_4 nanoparticles. The enhanced photocatalytic activity may be induced by the special accumulated feature of atoms on the facets, and this will be a major

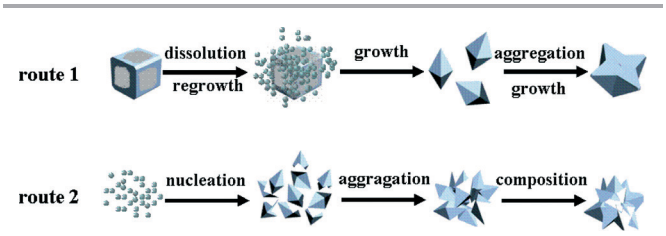

Scheme 1 Schematic illustration for the formation of the α-Ag_3VO_4 nanostructures. Route 1: nanostars and route 2: nanoflowers.

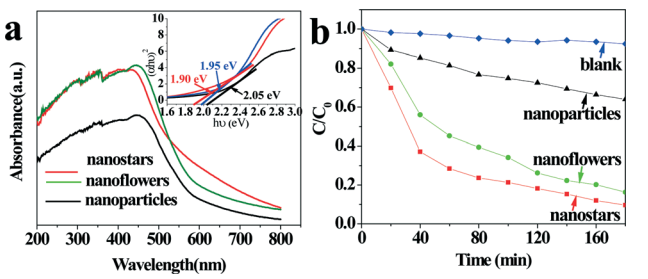

Fig. 3 (a) UV-vis absorption spectra and (b) photocatalytic activities of α-Ag_3VO_4 nanoparticles, nanostars and nanoflowers, with self-degradation of RhB as a blank.

area of our further work. This work is expected to provide a useful method to synthesize α-Ag_3VO_4 nanomaterials with regular morphology and high photocatalytic activity, and may realize the wide application of α-Ag_3VO_4 nanomaterials as a visible light photocatalyst.

Acknowledgements

This work was supported by the National Natural of Science Foundation of China (Grant No. 21073095 and 21371101) and 111 Project (B12015).

Notes and references

1 Y. S. Nam, A. P. Magyar, D. Lee, J. W. Kim, D. S. Yun, H. Park, T. S. P. Jr, D. A. Weitz and A. M. Belcher, *Nat. Nanotechnol.*, 2010, **5**, 340.
2 M. Barroso, A. J. Cowan, S. R. Pendlebury, M. Grätzel, D. R. Klug and J. R. Durrant, *J. Am. Chem. Soc.*, 2011, **133**, 14868.
3 S. K. Li, F. Z. Huang, Y. Wang, Y. H. Shen, L. G. Qiu, A. J. Xie and S. J. Xu, *J. Mater. Chem.*, 2011, **21**, 7459.
4 G. Trimarchi, H. W. Peng, J. Im and A. J. Freeman, *Phys. Rev. B: Condens. Matter*, 2011, **84**(1), 165116.
5 R. Konta, H. Kato, H. Kobayashi and A. Kudo, *Phys. Chem. Chem. Phys.*, 2003, **5**, 3061.
6 H. Xu, H. M. Li, L. Xu, C. D. Wu, G. S. Sun, Y. G. Xu and J. Y. Chu, *Ind. Eng. Chem. Res.*, 2009, **48**, 10771.
7 C. M. Huang, G. T. Pan, Y. C. M. Li, M. H. Li and T. C. K. Yang, *Appl. Catal., A*, 2009, **358**, 164.
8 M. R. Dolgos, A. M. Paraskos, M. W. Stoltzfus, S. C. Yarnell and P. M. Woodward, *J. Solid State Chem.*, 2009, **182**, 1964.
9 L. Etgar, T. Moehl, S. Gabriel, S. G. Hickey, A. Eychmüller and M. Grätzel, *ACS Nano*, 2012, **6**, 3092.
10 X. B. Chen and C. Burda, *J. Am. Chem. Soc.*, 2008, **130**, 5018.
11 Q. P. Wu and R. V. D. Krol, *J. Am. Chem. Soc.*, 2012, **134**, 9369.
12 K. Shiba, S. Sato and M. Ogawa, *J. Mater. Chem.*, 2012, **22**, 9963.
13 Q. Zheng, H. Kang, J. Yun, J. Lee, J. H. Park and S. Baik, *ACS Nano*, 2011, **5**, 5088.
14 C. W. Sun, S. Rajasekhara, Y. J. Chen and J. B. Goodenough, *Chem. Commun.*, 2011, **47**, 12852.
15 W. X. Zhang, M. Li, Q. Wang, G. D. Chen, M. Kong, Z. H. Yang and S. Mann, *Adv. Funct. Mater.*, 2011, **21**, 3516.
16 M. R. Gao, Z. Y. Lin, J. Jiang, H. B. Yao, Y. M. Lu, Q. Gao, W. T. Yao and S. H. Yu, *Chem.–Eur. J.*, 2011, **17**, 5068.
17 Y. H. Liang, L. Shang, T. Bian, C. Zhou, D. H. Zhang, H. J. Yu, H. T. Xu, Z. Shi, T. R. Zhang, L. Z. Wu and C. H. Tung, *CrystEngComm*, 2012, **14**, 4431.
18 T. R. Gordon, M. Cargnello, T. Paik, F. Mangolini, R. T. Weber, P. Fornasiero and C. B. Murray, *J. Am. Chem. Soc.*, 2012, **134**, 6751.
19 H. G. Yang, C. H. Sun, S. Z. Qiao, J. Zou, G. Liu, S. C. Smith, H. M. Cheng and G. Q. Lu, *Nature*, 2008, **453**, 638.
20 T. A. Albrecht, C. L. Stern and K. R. Poeppelmeier, *Inorg. Chem.*, 2007, **46**, 1704.
21 H. Wang, J. Gao, T. Q. Guo, R. M. Wang, L. Guo, Y. Liu and J. H. Li, *Chem. Commun.*, 2012, **48**, 275.
22 R. Dondi, W. Su, G. A. Griffith, G. Clark and G. A. Burley, *Small*, 2012, **8**, 770.
23 X. Wang, H. F. Wu, Q. Kuang, R. B. Huang, Z. X. Xie and L. S. Zheng, *Langmuir*, 2010, **26**, 2774.
24 H. T. S. Britton and R. A. Robinson, *J. Chem. Soc., Abstr.*, 1930, 2328.
25 T. Hirono, H. Koizumi and T. Yamada, *Thin Solid Films*, 1987, **149**, 85.
26 N. Bowden, A. Terfort, J. Carbeck and G. M. Whitesides, *Science*, 1997, **276**, 233.
27 J. Li and H. C. Zeng, *J. Am. Chem. Soc.*, 2007, **129**, 15839.
28 S. Sakthivel and H. Kisch, *Angew. Chem., Int. Ed.*, 2003, **42**, 4908.
29 Y. P. Bi, S. X. Ouyang, N. Umezawa, J. Y. Cao and J. H. Ye, *J. Am. Chem. Soc.*, 2011, **133**, 6490.
30 J. Pan, G. Liu, G. Q. Lu and H. M. Cheng, *Angew. Chem., Int. Ed.*, 2011, **50**, 2133.
31 F. Lu, W. P. Cai and Y. G. Zhang, *Adv. Funct. Mater.*, 2008, **18**, 1047.

